

Static and Dynamic Tensile Strain Yield Distinct ECM Remodeling and Signaling from Human Ligament Fibroblasts

Kenneth Tam¹, Jared Ong¹, Mai-Ly Wilkinson¹, Jonathan Joseph¹, Rogelio Castillo¹, Geovani Suarez¹, Keith Baar^{1,2}
¹University of California Davis, Davis, CA, ²VA Northern California Health Care System, Mather, CA
 kttam@ucdavis.edu

Disclosures: The authors have no disclosures.

INTRODUCTION: Injuries to the anterior cruciate ligament (ACL) are prevalent but recover poorly, resulting in long-term loss of physical function. Tensile loads critically regulate the biological processes that underly collagen remodeling and can promote recovery. However, the balance between loading parameters that facilitate recovery and those that accelerate degeneration remains poorly defined [1]. Recent evidence suggests that in viscoelastic materials, mechanotransduction in response to a given magnitude of load varies as a function of the pattern over time that the stimulus is applied [2]. As ligaments are viscoelastic, this concept can be applied and tested by comparing static versus dynamic tensile stimuli. Here, we tested the hypothesis that static and dynamic tensile stimuli elicit distinct remodeling mechanisms from human ligament fibroblasts. This hypothesis was tested in 3-dimensional ACL organoids (ACLO) at the level of acute mechanosensing, collagen content, collagen ultrastructure, crosslinking, and mechanical properties.

METHODS: Cells were isolated from remnants of human ACL from patients undergoing surgical ACL reconstruction (n=3 males; age:24±3y) following informed consent, using a protocol approved by the UC Davis Institutional Review Board. ACLOs (**Fig. 1A**) were formed by seeding 2.5x10⁵/mL ACL cells in 1 mL of fibrin gel around two β-tricalcium phosphate posts in a 35mm plate. ACLOs were fed every other day with growth media supplemented with 200 μM ascorbic acid, 50 μM proline, and 5 ng/ml of transforming growth factor-β1. For chronic remodeling studies, a custom bioreactor loaded ACLOs to 2% strain over 10 minutes every 6 hours for 6 days. Static loading was performed with 4 x 30s static holds at 2% strain separated by 2 minutes of rest, while dynamic loading was performed with a triangle waveform (**Fig. 1B**). Time under tension was matched between these two groups, and a third continuous dynamic loading group was tested to control for the strain-time integral. ACLOs were mechanically tested via ramp-to-failure, collagen content was measured via the hydroxyproline assay, matrix thermal properties were measured using differential scanning calorimetry, and collagen ultrastructure was quantified using transmission electron microscopy. To measure mechanosensing, ACLOs were collected 15 minutes after the first loading bout for western blot analysis. Data are expressed as the mean ± SD. Statistics were performed with 1-way ANOVA or student's t-tests with significance set at p<0.05.

RESULTS: After 6 days, stiffness increased relative to non-loaded controls with dynamic loading, and to a greater extent with static loading and continuous dynamic loading (**Fig 1C**). However, modulus only increased with static loading (**Fig. 1D**). Total collagen content generated by the ACL cells increased to the same extent in each of the static, dynamic, and continuous dynamic groups (**Fig. 1E**). There was no effect on the % collagen of dry mass. In terms of collagen ultrastructure, fibrils were disorganized and scattered in the control ACLOs (**Fig. 2A**), while the static-loaded ACLOs exhibited much more organized and clustered fibrils (**Fig 2B**). In the static load group, there was a greater proportion of small and large diameter fibrils, and appeared to begin forming a bimodal distribution of diameters (**Fig. 2C**). The fibrils in loaded ACLOs were also more densely packed (**Fig. 2D**). These adaptations corresponded with a greater gene expression ratio of Col1a1/Col3a1 (**Fig. 2E**), greater matrix thermal stability which suggests greater crosslinking (**Fig. 2F**), and greater MMP1 protein content (not shown). While ERK1/2 phosphorylation increases to the same extent in response to static and dynamic loading (**Fig. 3A**), myosin light chain (MLC) phosphorylation (**Fig. 3B**) and eukaryotic translation elongation factor 2 (EEF2) activation via dephosphorylation (**Fig. 3C**) only occurred with dynamic loading. In addition, phosphorylation of p70s6 kinase (p70s6k) increased only with static loading (**Fig 3D**).

DISCUSSION: We demonstrate fundamentally different remodeling responses by human ACL fibroblasts between dynamic and static loading. These differences in mechanical properties arose despite similar increases in total collagen content across these loading groups. The superior mechanical adaptations seen in the static loading group may be explained by the superior organization and composition (COL1/COL3) of this newly synthesized collagen. These differences may be mediated by the distinct remodeling signaling between dynamic and static tensile loading. Limitations of this study are that the tissues have had no prior loading history and that the response may reflect the response to undergoing these loads for the first time. Another limitation is the pH-buffered environment at 7.4, which may limit the collagen fibril assembly resulting from acidic and basic environments [3].

SIGNIFICANCE/CLINICAL RELEVANCE: While some features of remodeling in response to static and dynamic loading appear to overlap, different signaling mechanisms and matrix adaptations suggest that they are encoded distinctly. Mechanobiological therapies may exhibit similar patterns.

REFERENCES: 1. Killian et al. J Shoulder Elbow Surg. 2012. 2. Chaudhuri et al. Nature 2020. 3. Thomson et al. Biochem J 2000.

ACKNOWLEDGEMENTS: This research was supported by the Maury L. Hull Fellowship for Biomechanics Research.

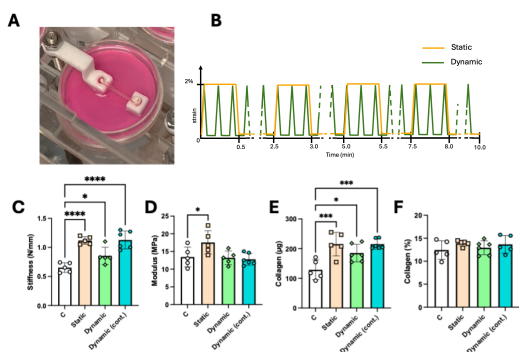


Fig. 1. Static and Dynamic Loads elicit distinct mechanical adaptations. (A) Representative image of ACLOs in tensile bioreactor. (B) Schematic of loading regimes. Schematic not to scale. (C) Stiffness, (D) Young's modulus, (E) Absolute collagen content, and (F) Relative collagen content after 6 days of loading. n=5-6 per group. *p<0.05, ***p<0.001, ****p<0.0001.

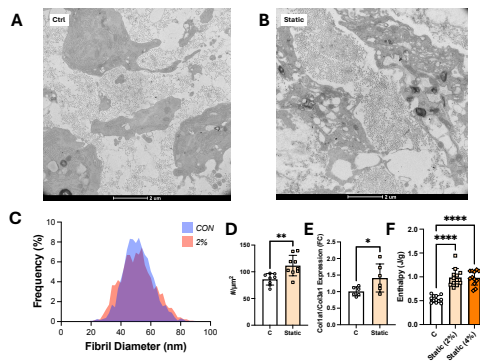


Fig 2. Collagen fibril structure changes after static loading. Cross-sectional transmission electron images (5300x) of (A) control and (B) statically loaded ACLOs. (C) Histogram of collagen fibril diameter (D) Collagen fibril density. n = 9 per group. (E) Ratio of gene expression of Col1a1/Col3a1. n=6 per group. (F) Matrix thermal stability with 2% and 4% static strain. n=12 per group. *p<0.05, **p<0.01, ****p<0.0001.

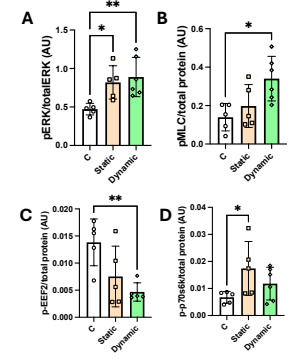


Figure 3. Acute mechanosensing varies between static and dynamic loading. Phosphorylation of (A) ERK1/2, (B) myosin light chain (MLC), (C) eukaryotic translation elongation factor 2 (EEF2), and (D) p70s6k. n=5-6 per group. *p<0.05, **p<0.01.